A Molecular Modeling Study of the Interactions between the Antiestrogen Drug Tamoxifen and Several Derivatives, and the Calcium-Binding Protein Calmodulin

Karen J. Edwards, Charles A. Laughton, and Stephen Neidle*

Cancer Research Campaign Biomolecular Structure Unit, The Institute of Cancer Research, Sutton, Surrey SM2 5NG, U.K.
Received October 21, 1991

The interactions of the antiestrogenic drug tamoxifen with the calcium-binding protein calmodulin have been studied by computerized molecular modeling methods. Sites in both the N and C domains of the protein have been established, with one in the C domain having the highest calculated enthalpy of binding. The residues involved in the sites have been detailed. Modeling studies are reported for six tamoxifen derivatives, and their calculated enthalpies of binding are compared with the ability of the analogues to inhibit calmodulin-dependent cyclic AMP phosphodiesterase (PDE) (Rowlands et al. *Biochem. Pharmacol.* 1990, *40*, 283-289). The poor binding properties of the piperazino and *C*-methyl derivatives are correctly predicted, whereas the superior affinity of 4-iodotamoxifen is not fully explained by the model.

Introduction

The synthetic drug tamoxifen is widely used in the treatment of hormone-sensitive breast cancer.[1,2] It may also be of use as a preventative agent against breast cancer, as indicated by a preliminary controlled feasibility study.[3] The classic view of the mechanism of action of tamoxifen is that it competes with the natural hormone estradiol for binding to sites on the estrogen receptor.[4,5] A number of studies have suggested that there are other macromolecules to which tamoxifen binds in addition to the estrogen receptor, some of which probably contribute to the antiproliferative activity[6,7] by means of their involvement in the signaling pathways maintaining cellular viability. In particular, the growth inhibitory action of tamoxifen on human breast cell lines has been suggested to correlate with inhibition of the calcium-dependent regulatory protein calmodulin,[8-10] and possibly with other components of the second messenger pathway such as protein kinase C.[11] However, it is the calmodulin effects which were of particular interest to us, especially in view of the possible synergism between the calmodulin and estrogen-receptor mediated effects, reflected in the ability of calmodulin to stimulate phosphorylation of the estrogen receptor protein.[12]

The binding of tamoxifen to calmodulin has recently been examined in detail, with a high-affinity and a low-affinity binding site being found.[13] Structure–activity relationships have been examined for a series of tamoxifen analogues with respect to their inhibition of calmodulin-dependent cyclic AMP phosphodiesterase,[14] which has demonstrated a correlation with cytotoxicity in MCF-7 cells. This study concluded that certain structural features of the tamoxifen molecule are important for binding, in particular a side chain capable of being protonated at physiological pH and its hydrophobic triphenylbutene moiety.

The present study examines the interactions of tamoxifen and several of its derivatives with calmodulin by means of molecular modeling techniques, in order to attempt to rationalize their binding behavior at the atomic level. We have examined a representative set of compounds that show maximal variation in substitution pattern and nature of side chain and for which calmodulin-inhibitory data are available.[14] We have also modeled the pyrrolidino analogue, for which there is as yet no data, and have predicted its likely activity. This approach has been made possible by the X-ray crystallographic analysis of calmodulin itself[15,16] in its calcium-bound form. Several qualitative molecular modeling studies have been reported for calmodulin–drug complexes, especially of the phenothiazene family,[17,18] as well as NMR studies on such com-

(1) Jordan, V. C.; Fritz, N. F.; Gottardis, M. M. Strategies for breast cancer therapy with antiestrogens. *J. Steroid Biochem.* 1987, *27*, 493-498.
(2) Mansi, J. L.; Smith, I. E. Endocrine therapy for breast cancer: mechanisms and new approaches. *Cancer Topics* 1989, *7*, 57-59.
(3) Powles, T. J.; Hardy, J. R.; Ashley, S. E.; Farrington, G. M.; Cosgrove, D.; Davey, J. B.; Dowsett, M.; McKinna, J. A.; Nash, A. G.; Sinnett, H. D.; Tillyer, C. R.; Treleaven, J. G. A pilot trial to evaluate the acute toxicity and feasibility of tamoxifen for prevention of breast cancer. *Br. J. Cancer* 1989, *60*, 126-131.
(4) Coezy, E.; Borgna, J. L.; Rochefort, H. Tamoxifen and metabolites in MCF-7 cells: correlation between binding to estrogen receptor and inhibition of cell growth. *Cancer Res.* 1982, *42*, 317-323.
(5) Jordan, V. C. Biochemical pharmacology of antiestrogen action. *Pharmacol. Rev.* 1984, *36*, 245-276.
(6) Sutherland, R. L.; Murphy, L. C.; Foo, M. S.; Green, M. D.; Whybourn, A. M.; Krozowski, Z. S. High-affinity anti-oestrogen binding site distinct from the oestrogen receptor. *Nature (London)* 1980, *288*, 273-275.
(7) Lipton, A.; Morris, I. D. Calcium anagonism by the antioestrogen tamoxifen. *Cancer Chemother. Pharmacol.* 1986, *18*, 17-20.
(8) Lam, H. Y. P. Tamoxifen is a calmodulin antagonist in the activation of c-AMP phosphodiesterase. *Biochem. Biophys. Res. Commun.* 1984, *118*, 27-32.
(9) Gulino, A.; Barrera, G.; Vacca, A.; Farina, A.; Ferretti, C.; Screpanti, J.; Dianzani, M. W.; Frati, L. Calmodulin antagonism and growth inhibiting activity of triphenylethylene antioestrogens in MCF-7 human breast cancer cells. *Cancer Res.* 1986, *46*, 6274-6278.
(10) Barrera, G.; Screpanti, I.; Paradisi, L.; Parola, M.; Ferretti, C.; Vacca, A.; Farina, A.; Dianzani, M. V.; Frati, L.; Gulino, A. Structure–activity relationships of calmodulin antagonism by triphenylethylene antiestrogens. *Biochem. Pharmacol.* 1986, *35*, 2984-2986.
(11) O'Brien, C. A.; Liskamp, R. M.; Soloman, D. H.; Weinstein, I. B. Triphenyl ethylenes: A new class of protein kinase C inhibitors. *J. Natl. Cancer Inst.* 1986, *76*, 1234-1246.
(12) Migliaccio, A.; Rotondi, A.; Auricchio, F. Calmodulin-stimulated phosphorylation of 17β-estradiol receptor on tyrosine. *Proc. Natl. Acad. Sci. U.S.A.* 1984, *81*, 5921-5925.
(13) Lopes, F.; Graca, M.; Vale, P.; Carvalho, A. P. Ca^{2+}-dependent binding of tamoxifen to calmodulin isolated from bovine brain. *Cancer Res.* 1990, *50*, 2753-2758.
(14) Rowlands, M. G.; Parr, I. B.; McCague, R.; Jarman, M.; Goddard, P. M. Variation of the inhibition of calmodulin dependent cyclic AMP phosphodiesterase amongst analogues of tamoxifen correlations with cytotoxicity. *Biochem. Pharmacol.* 1990, *40*, 283-289.
(15) Babu, Y. S.; Sack, J. S.; Greenhough, T. J.; Bugg, C. E.; Means, A. R.; Cook, W. J. Three-dimensional structure of calmodulin. *Nature (London)* 1985, *315*, 37-40.
(16) Babu, Y. S.; Bugg, C. E.; Cook, W. J. Structure of calmodulin refined at 2.2Å resolution. *J. Mol. Biol.* 1988, *204*, 191-204.

0022-2623/92/1835-2753$03.00/0

Table I. Molecular Mechanics Parameterization of Tamoxifen Analogues for AMBER (For the AMBER force field and definitions of symbols, see refs 22–24)

	bond parameters	
	K_r	r_{eq}
CA–I	450.000	2.05000
CA–OS	450.000	1.35500
CT–NT	367.000	1.47100
H3–NT	434.000	1.01000

	angle parameters	
	K_θ	θ_{eq}
CA–CA–I	70.000	120.000
CA–CA–OS	70.000	124.000
CT–CT–NT	80.000	111.200
HC–CT–NT	35.000	109.500
CT–NT–CT	35.000	109.500
CA–OS–CT	100.000	110.800
CA–OH–HO	100.000	110.800
OH–CA–CA	70.000	124.800

	nonbonded parameters		
I	2.35000	0.40000	0.00000

	torsion parameters			
	NTOR	$v/2$	δ	γ
CA–CA–OS–CT	1	0.00000	0.000	3.000
CA–CA–OH–HO	1	0.00000	0.000	3.000
HO–OH–CA–CA	1	0.00000	0.000	3.000
CT–CT–NT–CT	1	1.40000	0.000	3.000
CT–NT–CT–HC	1	1.40000	0.000	3.000
HC–CT–NT–H3	1	1.40000	0.000	3.000
CT–CT–NT–H3	1	1.40000	0.000	3.000

plexes.[19,20] All calmodulin-binding drugs appear to have a hydrophobic surface in common,[19,21] although the propeller shape of the triphenylbut-1-ene feature of tamoxifen suggests that it might have a distinct mode of binding.

Methods

Initial coordinates for calmodulin (in its calcium-bound form) and tamoxifen were obtained from their respective X-ray crystal structures as deposited in the Brookhaven and Cambridge databases. Atomic charges for tamoxifen and constructed analogues were calculated with the semiempirical molecular orbital program AMPAC[29] assigning a net overall charge of +1 to all analogues. All molecular mechanics calculations were performed at the all-atom level using the program AMBER 3.1.[22–24]

Table II. Dihedral Angles (deg) and Final Steric Energies (kcal mol^{-1}) for the Four Low-Energy Conformations of Tamoxifen[26]

	torsion angle[a]				
conformer	α	β	γ	δ	energy
1	47	66	72	47	-5.48
1_m	-45	-63	-71	-48	-5.47
2	47	62	-118	49	-5.22
2_m	-45	-60	118	-49	-5.20
crystal structure	50	64	-120	58	

[a] α = C8–C7–C17–C18, β = C8–C7–C1–C6, γ = C7–C8–C9–C10, δ = C7–C8–C11–C16.

A distance-dependent dielectric constant with $\epsilon = 4r_{ij}$ was used to compensate for lack of explicit solvent and a 9.5-Å residue-based nonbonded cut-off was applied to the electrostatic and van der Waals interactions.[25] All minimizations were performed to an rms gradient < 0.1 kcal mol^{-1} Å^{-1} allowing 100 cycles of steepest descent and then switching to conjugate gradient minimization.

Additional parameters required for tamoxifen and its analogues were obtained by comparison with analogous existing parameters, and are given in Table I.

All calculations were performed on an Alliant FX40/3 computer. Graphical displays and interactive manipulation were performed using the molecular modeling programs GEMINI[30] and MMS[31] running on a Silicon Graphics IRIS 3130 Workstation.

A full minimization and conformational search study on *trans*-tamoxifen[26] using the molecular mechanics program MMP2(85) has resulted in the location of two discrete low-energy conformations related by a 180° rotation about the ethyl group (conformers 1, 2) together with (non-superimposable) mirror images (conformers 1_m, 2_m) (Table II). The X-ray crystal structure of calmodulin[15,16] has shown that there are two hydrophobic clefts, one in each half of the protein molecule which are thought to represent the sites of interaction with drug molecules. We postulated that there are two binding sites for tamoxifen on calmodulin by direct analogy with results obtained for trifluoperazine–calmodulin binding in which it has been shown that two drug molecules bind to calmodulin.[17] Docked interaction complexes between calmodulin and tamoxifen were constructed on the basis of this, by fitting the hydrophobic portion of the drug into the grooves formed by the hydrophobic residues of calmodulin in such a way that the positively charged alkylamino side chain of the drug is in close proximity to negatively-charged acidic residues lining the hydrophobic pockets of the protein.

A solvent-accessible surface[27] was constructed for the calmodulin molecule and each of the four tamoxifen conformers were docked into the proposed binding sites using interactive graphics. The docking procedure was repeated several times with a number of different possible initial

(17) Strynadka, N. C. J.; James, M. N. G. Two trifluoperazine-binding sites on calmodulin predicted from comparative molecular modelling with troponin-C. *Proteins* 1988, *3*, 1–17.
(18) Höltje, H.-D.; Hense, M. A molecular modelling study on binding of drugs to calmodulin. *J. Comput.-Aided Mol. Des.* 1989, *3*, 101–109.
(19) Dalgarno, D. C.; Klevit, R. E.; Levine, B. A.; Scott, G. M.; Williams, R. J. P. The nature of trifluoperazine binding sites on calmodulin and toponin-C. *Biochim. Biophys. Acta* 1984, *791*, 164–172.
(20) Dalgarno, D. C.; Klevit, R. E.; Levine, B.; Williams, R. J. P.; Dobrowolski, Z. ^{1}H-NMR studies of calmodulin. Resonance assignments by use of tryptic fragments. *Eur. J. Biochem.* 1987, *138*, 281–289.
(21) Reid, D. G.; MacLachlan, L. K.; Gajjar, K.; Voyle, M.; King, R. J.; England, P. J. A proton nuclear magnetic resonance and molecular modelling study of calmidazolium (R24571) binding to calmodulin and skeletal muscle troponin-C. *J. Biol. Chem.* 1990, *265*, 9744–9753.
(22) Weiner, S. J.; Kollman, P. A.; Case, D. A.; Singh, U. C.; Ghio, C.; Alagona, G.; Profeta, S., Jr.; Weiner, P. A. A new force-field for molecular mechanical simulation of nucleic acids and proteins. *J. Am. Chem. Soc.* 1984, *106*, 765–783.
(23) Weiner, S. J.; Kollman, P. A.; Nguyen, P. T.; Case, D. A. An all atom force-field for simulations of proteins and nucleic acids. *J. Comput. Chem.* 1986, *7*, 230–252.
(24) Singh, U. C.; Weiner, P. K.; Caldwell, J.; Kollman, P. A. AMBER (Version 3.1) 1988, Department of Pharmaceutical Chemistry, University of California, San Francisco.
(25) Whitlow, M.; Teeter, M. M. An empirical examination of potential energy minimization using the well-determined structure of the protein Crambin. *J. Am. Chem. Soc.* 1986, *108*, 7163–7172.
(26) Edwards, K. J.; Laughton, C. A.; Neidle, S. A note on the conformational flexibility of the antiestrogenic drug tamoxifen; preferred conformations in the free state and bound to the protein calmodulin. *Acta Crystallogr.* 1992, in press.
(27) Connelly, M. L. Solvent-accessible surfaces of proteins and nucleic acids. *Science* 1983, *221*, 709–713.

Table III. Energy Analysis for the Best Docked Models after Initial Drug Minimization (The energies here are after the second, constrained minimization)

model	conformer of drug	E_{tam}	$E_{pert(tam)}$	E_{cam}	$E_{pert(cam)}$	E_q	E_{vdw}	$\Delta E_{binding}$
				Site I (C-terminus)				
Ia	1	33.3	0.4	5038.9	-10.4	-6.5	-16.3	-32.8
Ib	1	33.8	1.0	5047.9	-1.4	-9.9	-16.9	-27.2
Ic	1	36.7	3.8	5060.9	11.6	-8.4	-18.2	-11.2
Id	1_m	39.7	6.8	5047.0	-2.3	-10.6	-15.3	-21.4
				Site II (N-terminus)				
IIa	2	34.4	0.7	4919.8	7.0	-5.0	-21.6	-18.9
IIb	1_m	39.1	5.4	4915.4	2.6	-6.4	-17.6	-16.0
IIc	1_m	42.4	8.7	4914.0	1.2	-4.9	-18.3	-13.3
IId	2_m	41.5	7.8	4921.5	8.7	-6.3	-20.9	-13.1

orientations for each conformer in order to explore all likely binding geometries. This resulted in a total of twenty initial docked complexes, nine for the C-terminal site (of which there were three each for conformers 1 and 2, and two for conformer 2_m and one for conformer 1_m), and 11 for the N-terminal site (of which there were three models each for conformers 1, 1_m, and 2 and two models for conformer 2_m).

Each docked interaction complex was then subjected to a partial minimization allowing unrestrained movement for tamoxifen and holding the calmodulin molecule rigid, 500–950 cycles being required for convergence. Interaction energies were calculated for the drug, protein, and drug/protein complex and the binding energy, $\Delta E_{binding}$, obtained as follows:

$$\Delta E_{binding} = E_{vdw} + E_q + E_{pert}$$

where E_{vdw} and E_q are the van der Waals and electrostatic contributions to the interaction energy, and E_{pert} is the perturbation energy (i.e. the difference in energy between the ground-state conformation of the individual molecules and the intramolecular energy of the complex after binding).

On the basis of their binding energies and a visual inspection of the minimized model the best eight models (four from each site) were subject to further minimization in which now only the protein backbone atoms were constrained. For this constrained minimization the two domains were treated separately, allowing unrestrained movement in side chains of residues 75–147, for the C-terminal, and the side chains of residues 1–80, for the N-terminal, 800–2900 cycles being required for convergence. Interaction and binding energies were calculated as before (Table III). These binding energies have no entropic component and are thus most correctly described as binding enthalpies. A calculation of the interaction energy between tamoxifen and each residue was performed for each model in order to deduce which residues were important in binding. A minimum interaction energy of ca. -1.0 kcal/mol was taken as a significant contribution. The components (electrostastic and van der Waals) of the interaction were also calculated.

The molecular structures of several analogues of tamoxifen were also examined. These modifications comprised side-chains variants (diethylamino, piperazino, and pyrrolidino in place of dimethylamino), 4-substitutions (iodo and hydroxyl), and replacement of the ethyl substituent by methyl (Figure 1). These were constructed graphically and the four dihedral angles (α, β, γ, δ) (Table II) rotated to give low-energy conformers equivalent to those obtained for *trans*-tamoxifen. [In the case of the piperazino analogue, monoprotonation was assumed on one of the two ring nitrogen atoms, in accordance with the known monoprotonation of a piperazine ring at the pH of the calmodulin inhibition studies (pH 7.4).[14]] In all cases,

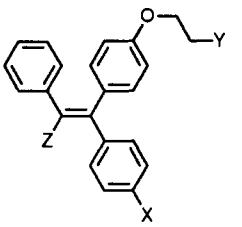

X = H; Y = NMe_2; Z = Et tamoxifen
X = H; Y = NEt_2; Z = Et *N,N*-diethyl derivative
X = H; Y = N⟨⟩NH; Z = Et piperazino derivative
X = H; Y = N⟨⟩; Z = Et pyrrolidino derivative
X = I; Y = NMe_2; Z = Et 4-iodo derivative
X = OH; Y = NMe_2; Z = Et 4-hydroxy derivative
X = H; Y = NMe_2; Z = Me *C*-methyl derivative

Figure 1. The molecular formulae of the tamoxifen derivatives examined in this study. The four conformational angles varied are indicated.

monoprotonation of the basic side chain was assumed, in accordance with the pH of the calmodulin-inhibition studies (pH 7.4).[14] For the piperazino analogue, two situations were modeled: protonation at either the proximal or terminal nitrogen atom. In addition, a number of different conformations for the piperazino ring for both protonated forms were explored in order to obtain the lowest ground-state energy.

Each of the analogues in the appropriate conformation was substituted for tamoxifen in the four best calmodulin/tamoxifen complexes (i.e. two from each site describing different orientations). The new calmodulin/drug models were then partially minimized as before, allowing the drug unrestrained movement while keeping calmodulin fixed (300–1500 cycles being needed for convergence depending on the derivatives). The binding energies and residue interaction energies were calculated for each complex as previously described (Table IV, sections a–f).

Results

Tamoxifen. The drug-binding sites on calmodulin in the active Ca^{2+} bound form are characterized by a well-defined groove in each domain. Figures 2a,b shows the solvent-accessible surface of the cleft in each domain. In addition to the large groove in the C-terminal domain, there is a small distinct cavity formed by the side chains of residues met144 and met145. The corresponding secondary cavity in the N-terminus which would be formed by residues met71 and met72 is not, however, clearly defined. The hydrophobic patches are surrounded by acidic residues on the edges of the dumbbells and also by those residues clustered around the central helix.

Molecular modeling has resulted in the prediction of a number of possible orientations for tamoxifen in each site, in which the charged side chain interacts either with the

Table IV. Energy Analysis for the Tamoxifen Analogues

Model	E_{drug}	$E_{pert(drug)}$	E_{cam}	$E_{pert(cam)}$	E_q	E_{vdw}	$\Delta E_{binding}$
			(a) The *N,N*-Diethyl Analogue				
Ia	38.6	2.7	5038.9	-10.4	-5.7	-16.4	-29.8
Ib	36.5	0.6	5047.9	-1.4	-8.3	-16.1	-25.2
IIa	36.0	0.1	4919.9	7.1	-4.0	-19.7	-16.5
IIb	49.0	13.1	4915.6	2.8	-5.6	-16.2	-5.9
			(b) The Piperazino Analogue (Proximally Protonated)				
Ia	47.5	5.2	5038.9	-10.4	-5.7	-17.3	-28.2
Ib	46.6	4.3	5047.9	-1.4	-9.4	-18.3	-24.8
IIa	46.7	4.4	4919.9	7.1	-3.9	-19.4	-16.1
IIb	50.0	7.7	4915.6	2.8	-6.9	-21.6	-13.5
			The Piperazino Analogue (Terminally Protonated)				
Ia	52.9	11.9	5038.9	-10.4	-6.2	-16.2	-21.1
Ib	52.3	11.3	5047.9	-1.4	-11.8	-18.2	-20.0
IIa	51.9	10.9	4919.9	7.1	-5.0	-19.4	-10.7
IIb	64.8	23.8	4915.6	2.8	-10.6	-20.8	-0.5
			(c) The 4-Iodo Analogue				
Ia	34.6	1.7	5038.9	-10.4	-5.7	-17.5	-31.9
Ib	33.1	0.2	5047.9	-1.4	-9.1	-17.3	-27.6
IIa	33.8	0.9	4919.9	7.1	-4.0	-19.9	-15.9
IIb	45.4	12.5	4915.6	2.8	-5.0	-16.2	-5.9
			(d) The 4-Hydroxy Analogue				
Ia	34.1	2.1	5038.9	-10.4	-5.8	-16.7	-30.8
Ib	32.8	0.8	5037.9	-1.4	-9.6	-18.5	-28.7
IIa	32.8	0.3	4919.9	7.1	-4.3	-19.8	-16.7
IIb	40.6	8.6	4915.6	2.8	-6.6	-18.3	-13.5
			(e) The *C*-Methyl Analogue				
Ia	37.2	5.2	5038.9	-10.4	-5.6	-13.7	-24.5
Ib	31.9	-0.1	5047.9	-1.4	-9.3	-15.9	-26.7
IIa	31.6	-0.4	4919.9	7.1	-3.8	-17.7	-14.8
IIb	38.2	6.0	4915.6	2.8	-5.9	-18.8	-15.9
			(f) The Pyrrolidino Analogue				
Ia	46.5	4.2	5038.9	-10.4	-5.5	-16.5	-28.2
Ib	44.0	1.7	5047.9	-1.4	-9.2	-18.0	-26.9
IIa	43.8	1.5	4919.9	7.1	-3.8	-19.2	-18.7
IIb	52.4	10.1	4915.6	2.8	-6.5	-19.9	-9.2

Table V. Torsion Angles of Tamoxifen Conformers in Drug-Bound Complexes after Minimization

		angle, deg			
model	conformer	α	β	γ	δ
Ia	1	26	47	66	38
Ib	1	15	50	64	29
IIa	2	40	54	-119	32
IIb	1_m	-30	-56	-40	-39

charged residues clustered around the helix or those at the periphery of the dumbbell. Table III details the final binding energies arising from these models after minimization. All of the four best models in the C-terminus site involve conformer 1 (or its mirror image). The best three of these have higher $\Delta E_{binding}$ than the N-terminal ones, with the differences being highly significant for the best two models Ia, Ib, compared to the rest.

A general feature of all low-energy interaction models is that the ethyl group is well-embedded in the small subsidiary hydrophobic cavity, and with the phenyl rings fitting snugly into the groove formed by the hydrophobic residues. The positively charged alkylamino side chain is then positioned in such a way as to be able to interact with negatively charged residues surrounding the pocket.

A comparison of the initial (Table II) and final (Table V) torsion angles for tamoxifen in the docked complexes shows an appreciable shift away from the optimum positions for the drug alone. The shifts in angles shown by conformer 2 are not as noticeable as those for 1. Conformer 2_m, however, shows quite large shifts, especially for the γ dihedral angle which has moved from an initial position away from the surface to a position in which it is able to interact favorably with hydrophobic residues in the binding site. The strong electrostatic and hydrophobic interactions in the bound complexes therefore overcome the effect of energetically unfavorable orientations of tamoxifen. This is then reflected in the size of the drug perturbation energy; when this is large (cf. model IIb), the changes in conformation are greatest. The two best models from each domain are described in further detail here.

In the C-terminal domain, the binding site of model Ia has the hydrophobic part of the tamoxifen molecules interacting with the side chains of residues ile85, phe92, ala147, met109, met124, met144, and met145 (which constitute the hydrophobic pocket in calmodulin) (Figures 3 and 4a). The charged side chain is oriented toward the α-helix linking the two domains of the dumbbell where it has interactions with glu82 and glu84.

In model Ib (Figure 5) the tamoxifen molecule has swung round, allowing its side chain to interact with a number of different acidic residues on the edges of the dumbbell, i.e. glu120, glu123, glu114, glu119, and glu127. The electrostatic component of this interaction is more favorable than for model Ia. The ethyl group is still embedded in the small cavity, and the phenyl groups lie along the grooves of the pocket interacting with the side chains of residues phe92, met109, met124, met144, and met145. The calculated binding enthalpy for this model is significantly less than for model Ia, largely because of the latter's more favorable protein perturbation energy.

In the N-terminal hydrophobic patch, the binding site of model IIa (Figures 6 and 4b) shows interactions of the

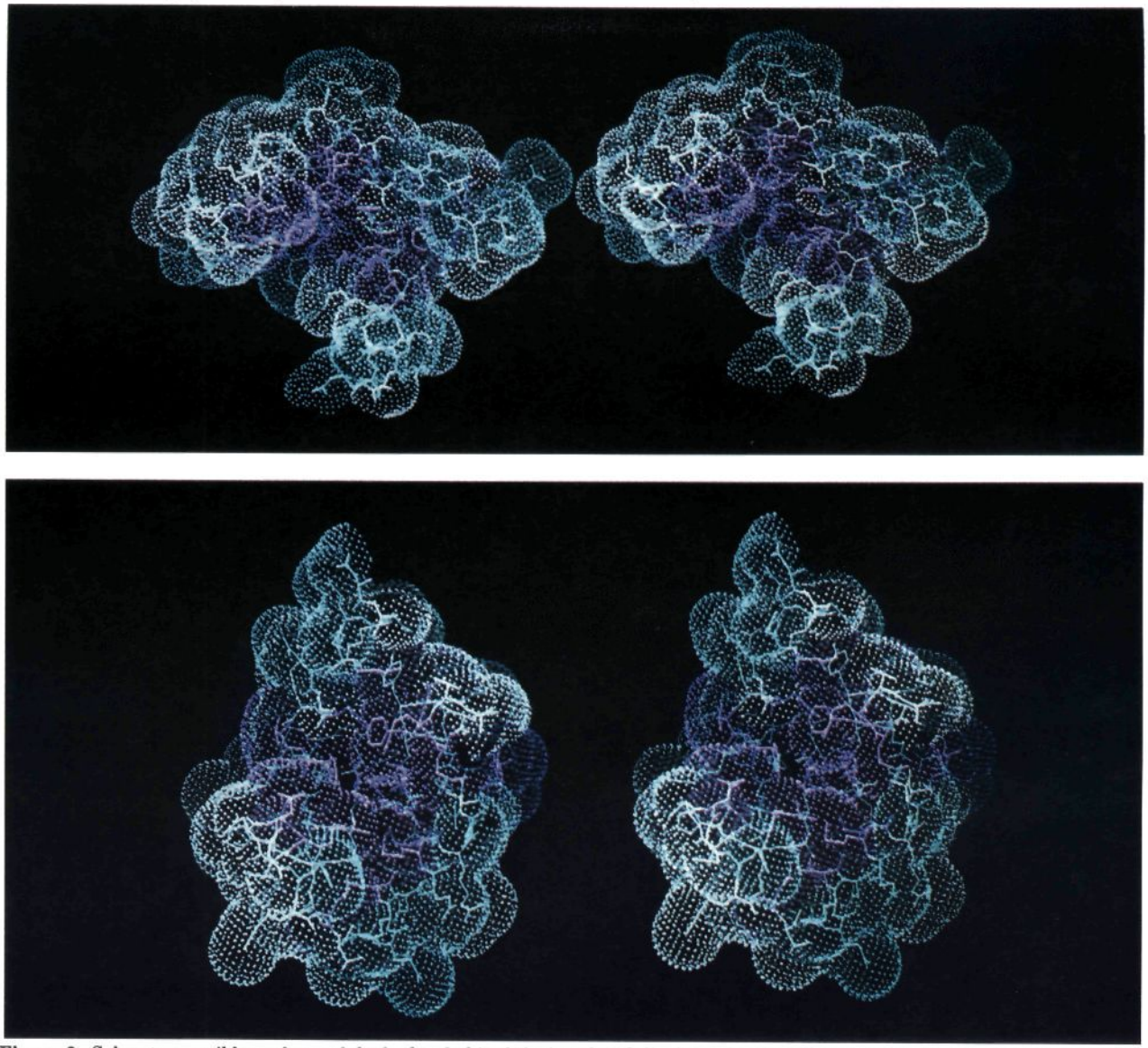

Figure 2. Solvent-accessible surfaces of the hydrophobic clefts in calmodulin (a, top) for the C-terminus domain, (b, bottom) for the N-terminus domain.

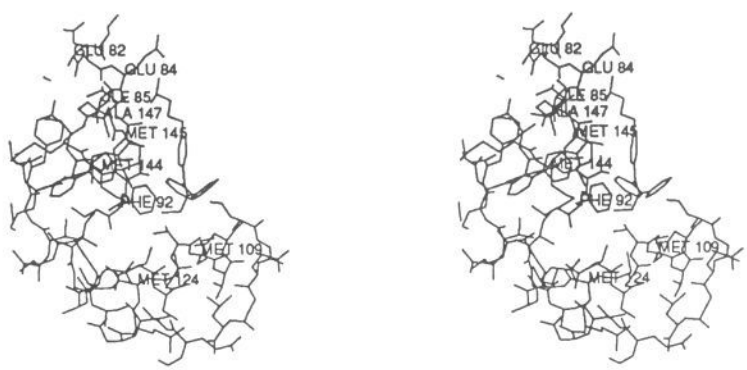

Figure 3. Computer-drawn plot of the binding site of model Ia, showing the residues in contact with the tamoxifen molecule.

hydrophobic groups of the drug with the residues phe12, phe19, phe68, leu18, leu39, val35, met36, and met72. The charged side chain of the drug interacts with glu11 and glu14 which extend off the helix. This model (together with the other N-terminus models in Table III) all produce unfavorable protein perturbation energies, resulting in reduced $\Delta E_{\text{binding}}$ values compared to the C-terminus models.

Model IIB (Figure 7) again shows an alternative arrangement in which the charged side chain interacts with the acidic residues glu54, glu47, and asp50 on the edge of the dumbbell. The hydrophobic residues involved in the interaction are phe19, phe68, leu32, met36, met51, met71, met72, and lys75. In this case, however, in contrast to the C-terminal binding sites, the whole molecule has moved to a different location within the groove and the ethyl

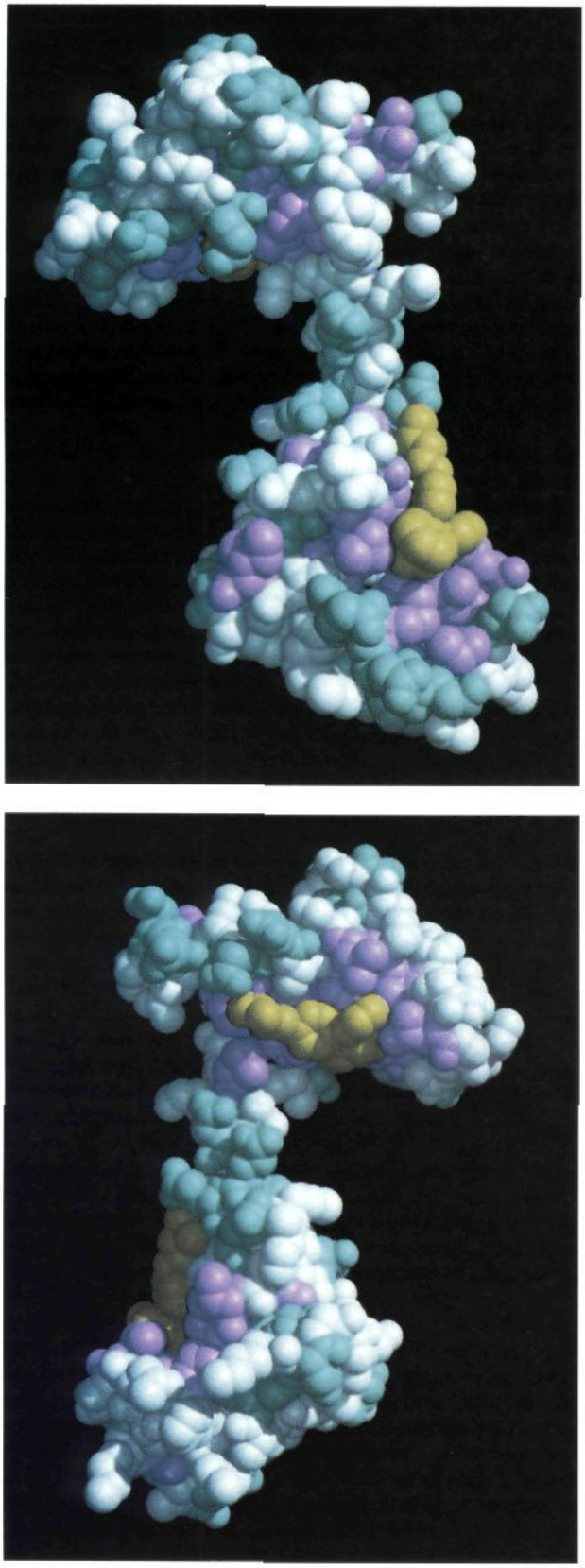

Figure 4. Space-filling representations of two molecules of tamoxifen bound to calmodulin, oriented to show (a, top) model Ia (C-terminus, bottom) and (b, bottom) model IIa (N-terminus, top). Tamoxifen is in yellow, the hydrophobic regions are in magenta, and the positively charged residues are in cyan. The figures were drawn with the MIDAS program (University of California, San Francisco).

group now interacts with completely different residues.

Tamoxifen Analogues. In each case, four models were examined, two each in the C- and N-termini.

All analogue models in sites Ia, Ib, and IIa show consistent results on changing various groups on the original tamoxifen molecule. Apart from some variation in the position of the charged side chain, there was no appreciable movement in the minimized position of the hydrophobic portion of the drug analogues.

There are a number of discrepancies for site IIb models compared to the original tamoxifen one, with minimization of the tamoxifen analogues showing varying shifts away from the original tamoxifen minimized position, indicating the involvement of unfavorable interactions. In view of this complication, we have restricted the comparison between analogues in the N-terminal domain to models of type IIa.

All analogues have calculated binding energies for the C-terminus domain that are significantly greater than for the N-terminus domain (Table IV, sections a–e). Contacts to residues are overall the same as those proposed for the tamoxifen models with some additional contacts being found in several cases. In model IIa for the *N,N*-diethyl analogue there is interaction with met76, glu83, and asp80 with the loss of the important interaction to glu14. This analogue has models Ia and Ib showing loss of interaction with residues met124 and glu119, respectively. For the piperazino analogue models, in Ia there are no longer contacts to residues met124, phe92, and glu82, and in model Ib glu119 is no longer involved, but there are additional contacts to leu116 adn ala147. Model IIa no longer has interaction with lys75 but has instead a contact to met76.

The proposed models for the *C*-methyl analogue show reduced interactions, largely as a result of replacing the *C*-ethyl by a methyl group, which has resulted in a decrease in van der Waals energy. Model Ib retains all contacts found for the tamoxifen model but model Ia has lost contacts to residues ile85 and met124, while model IIb is missing contacts to residues val35, met36, and glu14; there are additional interactions to met76 and asp80.

Contacts to residues in models Ia, Ib, and IIb are the same for the pyrrolidino analogue as those observed for tamoxifen itself. There are additional contacts for model IIa, to Met76, Asp80, and Glu83.

Analysis of the 4-iodo analogue was expected to produce increased binding energy due to the substitution at the 4-position by a large hydrophobic group, iodine. This was not found, and binding energies obtained for these models are similar to that for tamoxifen, as indeed are the residue interactions.

A significant decrease in binding affinity was to be expected for the 4-hydroxyl derivative as a result of decreased hydrophobicity at the 4-position but the calculated binding energies do not reflect this. As with the iodo analogue, residues involved in the interaction are essentially the same as those predicted for the tamoxifen models.

Table VI summarizes the calculated binding enthalpies for these analogues and compares them with the IC_{50} values for inhibition of the calmodulin-dependent cyclic AMP phosphodiesterase. None of the compounds gave any significant inhibition of the calmodulin-independent cyclic AMP phosphodiesterase activity when assayed at final concentrations of 10 and 20 μM.[14] The calculated $\Delta E_{binding}$ energies for the piperazino analogue models show significantly different results depending on the protonation site. The proximally protonated analogue shows slightly reduced $\Delta E_{binding}$ values in all sites compared to tamoxifen

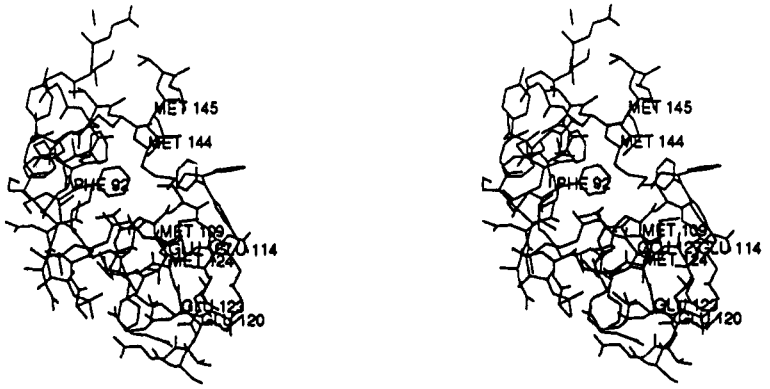

Figure 5. Computer-drawn plot of the binding site of model Ib, showing residues in contact with the drug.

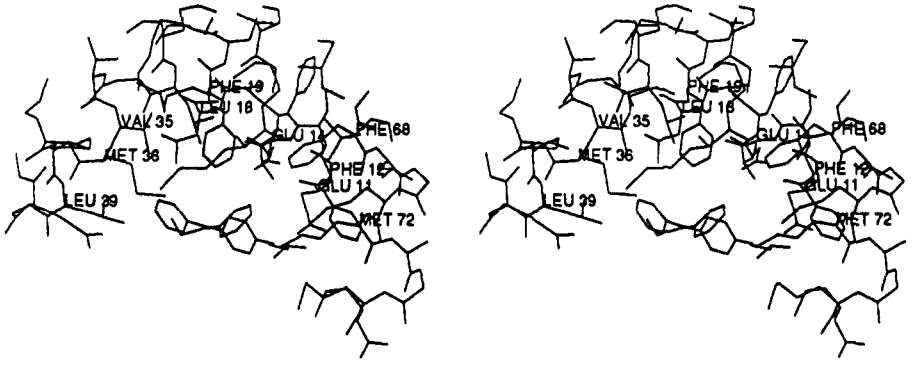

Figure 6. Plot of the binding site of model IIa.

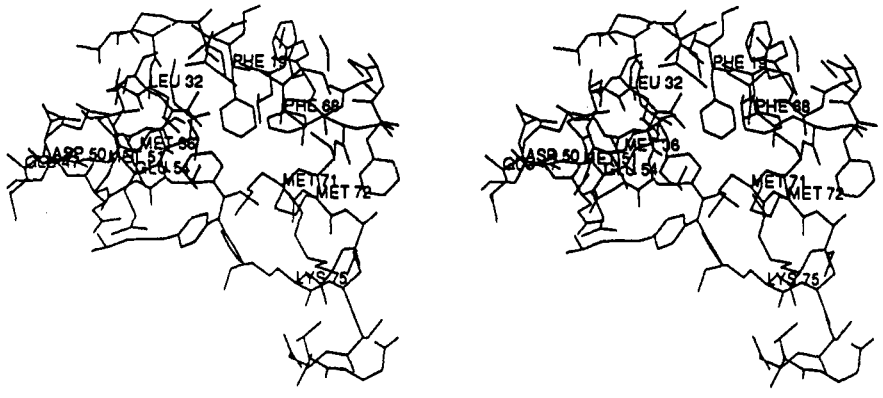

Figure 7. Plot of the binding site of model IIb.

Table VI. Comparison of Binding Energies with IC_{50} Values for Inhibition of Calmodulin-Dependent cAMP-PDE, for the Tamoxifen Analogues[14]

analogue	$\Delta E_{binding}$, kcal/mol				IC_{50}, μM (±SD for triplicate determinations)
	Ia	Ib	IIa	IIb	
tamoxifen	−32.8	−27.2	−18.9	−16.0	6.75 ± 1.06
N,N-diethyl	−29.8	−25.2	−16.5	−5.9	10.0 ± 1.2
4-iodo	−31.9	−27.6	−15.9	−5.9	2.3 ± 0.42
4-hydroxy	−30.8	−28.7	−16.7	−13.5	19.0 ± 2.85
C-methyl	−24.5	−26.7	−14.8	−15.9	20.0 ± 2.0[a]
pyrrolidino	−28.2	−26.9	−18.7	−9.2	*b*
piperazino (proximal protonation)	−28.2	−24.8	−16.1	−13.5	
piperazino (terminal protonation)	−21.1	−20.0	−10.7	−0.5	>50.0

[a] McCague, R.; Rowlands, M. G. Personal communication. [b] Results not available.

and in general lower values than those obtained from the pyrrolidino analogue; however, the terminally protonated analogue has greatly reduced $\Delta E_{binding}$ energies, lower even than the *C*-methyl analogue, and reflecting its poor IC_{50} assay value. Those for the *N,N*-diethyl and *C*-methyl analogue are similarily reduced, although to a lesser extent.

Two analogues show contradictory behavior, which does not fall into the overall pattern of results. The 4-hydroxyl has calculated $\Delta E_{binding}$ values that are not significantly different from those of the parent compound, yet its IC_{50} value is much higher, indicative of weaker binding. The $\Delta E_{binding}$ values for the 4-iodo derivative do not reflect, on

the other hand, its superior IC_{50} value. Experimental binding data is not as yet available for the pyrrolidino analogue. Our results predict an IC_{50} value for it between that of tamoxifen itself and that for the *N,N*-diethyl analogue.

Discussion

The interaction models for tamoxifen with calmodulin, particularly for site I on the C-terminal domain, strongly suggest that the ethyl group of the drug is important for activity and indeed there is experimental evidence to show that if replaced by a methyl group there is significant loss of activity. This is further substantiated by the present molecular modeling results (Tables IV, section e, and VI).

We have recently shown[26] that tamoxifen itself has two distinct low-energy conformers, together with their mirror images. The two forms differ in the orientation of the ethyl group, and are approximately equi-energetic with two low barriers to rotation between them, of 4.3 and 2.0 kcal mol^{-1}. The numerous crystal structures of tamoxifen and its analogues (for example, ref 28) all shown just one orientation of the ethyl group with a γ value of ca. $-120°$. Our energy calculations[26] on tamoxifen, with the finding of alternative equi-energetic conformations, suggested that all should be considered in binding to a macromolecular site. Tables III and V show that there is clearly one preferred orientation for the ethyl group of tamoxifen in its best calmodulin binding site (Ia), and that this is not that observed in the crystal structures of the free drug. This suggests that care should be taken when deriving structure–activity relationships for tamoxifen analogues based on their crystal-structure data.

Examination of Tables II and V show that there are significant decreases in the four tamoxifen torsion angles α–δ, of up to 20°, on going from in vacuo to the bound state. This flattening of the molecule is a consequence of its snug fit into the hydrophobic grooves in all models, with the hydrophobic surface contacts being optimal. These small changes are achieved with only a very small energy cost (Table III), which are more than compensated for by increased van der Waals energy contributions.

Experimental evidence for effective inhibition has shown that the aminoethoxy side chain should not be too bulky and should be positively charged. Results obtained from molecular modeling with the piperazino, pyrrolidino, and *N,N*-diethyl analogues, all show the effect of these bulkier groups on the binding energy and furthermore show the importance of the electrostatic contribution to calmodulin antagonism. On this basis, we would not expect the *N*-oxide analogue to have a low binding energy; the negatively charged polar oxygen atom would necessarily be in an acidic environment. This compound does have low activity.[14] The results obtained with the two possible protonated sites on the piperazino analogue are consistent with terminal nitrogen protonation occurring in solution, and hence in the biological assay, which gives a lower binding affinity for this analogue.

The importance of hydrophobic forces has been highlighted by experimental findings that varying the hydrophobicity for the 4-substituent has a profound effect on the IC_{50} value.[14] Increased hydrophobicity of the substituent led to more effective inhibition by the drug molecule. This is a result which our modeling studies cannot satisfactorily explain, with the 4-iodo derivative showing no significant improvement in binding energy compared to tamoxifen and the 4-hydroxyl derivative showing no significant decrease. The cause of these failures may lie in our treatment of solvation. We have not included explicit solvent in our calculations for reasons of computational expense. However, it may be that for these 4-substituted analogues the energies associated with desolvation are significantly different. As desolvation of the hydroxyl group may be expected to be less favorable than for an iodo group, the inclusion of such a term would tend to correct our calculated values. We cannot also discount the fact that comparisons between calculated binding enthalpies and IC_{50} values are semiquantitative at best, since there is no direct thermodynamic or other relation between these quantities. The assay for tamoxifen analogues is an indirect one. It measures calmodulin antagonism rather than direct calmodulin binding, and although it is a biochemically functional assay and therefore a relevant one, factors other than pure calmodulin binding cannot be discounted. The fact that tamoxifen and an analogue have both been shown to be competitive inhibitors of calmodulin-stimulated phosphodiesterase activity[8,14] by means of double-reciprocal plot analysis strongly suggests that the IC_{50} values given here are meaningful indications of relative binding abilities in the absence of more direct data. We conclude that the comparison between experiment and theory (Table VI) is qualitatively satisfactory, suggesting that the molecular modeling approach may be useful in the prediction of new taxoxifen analogues with enhanced affinity for calmodulin, apart for 4-substituted ones (Edwards et al., in preparation).

The finding in this study that tamoxifen is predicted to bind significantly more strongly to the C-terminus hydrophobic domain than to the N-terminus one is entirely consistent with recent findings of two classes of binding site for the drug[13] with apparent dissociation constants of about 5 nM and 9 μM even though there is as yet no direct evidence linking these two with our assignments. The affinity of trifluoperazine for the C-terminus has been reported to be at least 1 order of magnitude greater than for the N-terminus,[19] again consistent with our modeling studies.

There is as yet no detailed X-ray crystal structure of any drug–calmodulin complex. However, there is strong experimental evidence that the model presented here is a reasonable one. The analysis of the native protein[16] reported some soaking experiments with trifluoperazine; some electron density was seen in the region of the hydrophobic clefts, but was too unclear to be fitted to the drug molecule. Comparative molecular modeling with this drug based on the crystal structure of troponin C[17] has suggested that the hydrophobic rings of trifluoperazine fit into the grooves at the C-terminus formed by val91, val108, leu112, met109, phe92, met144, met145, and ala88, and at the N-terminus by val35, leu39, met36, leu18, met71, met72, phe19, and ala15. These correspond to sites Ia and IIa in the present study for tamoxifen. A combined NMR and molecular modeling study of the calmidazolium–calmodulin complex[21] has highlighted the importance of residues phe12, phe19, and phe68 in the N-terminus and phe92, phe89, phe141, tyr138, and tyr99 in the C-terminus. Again, bearing in mind the considerable structural diversity between this drug and tamoxifen, the binding sites are

(28) Kuroda, R.; Cutbush, S.; Neidle, S.; Leung, O.-T. Structural studies on some tamoxifen derivatives. *J. Med. Chem.* 1985, *28*, 1497–1503.
(29) Quantum Chemistry Program Exchange, No. 506, Department of Chemistry, Indiana University.
(30) Beveridge, A., available from CRC Biomolecular Structure Unit, The Institute of Cancer Research, Sutton, Surrey SM2 5NG, U.K.
(31) Dempsey, S. D., Department of Chemistry, University of California, San Diego, La Jolla, CA 92096.

close to sites Ia and IIa here.

Acknowledgment. This work was supported by the Cancer Research Campaign. K.J.E. is a Cancer Research Campaign Research Student. We are grateful to Professor M. Jarman and Dr. M. G. Rowlands for many useful discussions.

Registry No. Tamoxifen, 10540-29-1; tamoxifen *N,N*-diethyl derivative, 97818-91-2; tamoxifen piperazino derivative, 97818-85-4; tamoxifen pyrrolidino derivative, 15917-44-9; tamoxifen 4-iodo derivative, 116057-66-0; tamoxifen 4-hydroxy derivative, 65213-48-1; tamoxifen *c*-methyl derivative, 15917-50-7.

Quinoline Antifolate Thymidylate Synthase Inhibitors: Variation of the C2- and C4-Substituents

Peter Warner,*,† Andrew J. Barker,† Ann L. Jackman,‡ Kenneth D. Burrows,† Neal Roberts,† Joel A. M. Bishop,‡ Brigid M. O'Connor,‡ and Leslie R. Hughes†

Department of Chemistry, ICI Pharmaceuticals, Mereside, Alderley Park, Macclesfield, Cheshire SK10 4TG, UK, and Institute of Cancer Research, 15 Cotswold Road, Sutton, Surrey SM2 5NG, UK. *Received December 16, 1991*

Modifications to the bicyclic ring system of the potent thymidylate synthase (TS) inhibitor *N*-[4-[*N*-[(2-amino-3,4-dihydro-4-oxo-6-quinazolinyl)methyl]-*N*-prop-2-ynylamino]benzoyl]-L-glutamic acid (1, CB3717) have led to the synthesis of a series of quinoline antifolates bearing a variety of substituents at the C2 and C4 positions. In general the synthetic route involved the coupling of the appropriate diethyl *N*-[4-(prop-2-ynylamino)benzoyl]-L-glutamate with a disubstituted 6-(bromomethyl)quinoline followed by deprotection using mild alkali. The compounds were tested as inhibitors of partially purified L1210 TS. As a measure of cytotoxicity, the compounds were tested for their inhibition of the growth of L1210 cells in culture. Good enzyme inhibition and cytotoxicity were found for compounds containing chloro, amino, or methyl substituents at the C2 position with chloro or bromo substituents at C4. The effect on enzyme inhibition of varying the N10 substituent of **2h** was similar to that observed in the quinazolinone-containing antifolates, indicating that the quinoline compounds may be interacting with the enzyme in a similar way to the quinazolinones. Also, the introduction of a 2'-fluoro substituent into the benzoyl ring of several of the quinoline antifolates led to an increase in both TS inhibition and the inhibition of L1210 cell growth. These data demonstrate that the N3-H of the pyrimidine ring of the quinazolinone antifolates is not required for binding to TS if appropriate substituents are placed at the C2 and C4 positions of the bicyclic ring system.

Introduction

The 2-aminoquinazoline antifolate *N*-[4-[*N*-[(2-amino-3,4-dihydro-4-oxo-6-quinazolinyl)methyl]-*N*-prop-2-ynylamino]benzoyl]-L-glutamic acid (CB3717, 1) is a potent inhibitor ($K_i \approx 3$ nM) of both murine and human thymidylate synthase (TS, EC 2.1.1.45) and shows antitumor activity in some animal models.[1-7] Phase I/II clinical studies with 1 demonstrated responses in patients, particularly those with breast, ovarian, and liver cancer.[8-14] However, the compound caused unacceptable side effects, in particular, unpredictable liver and dose-limiting life-threatening kidney toxicities. Studies indicated that at least the nephrotoxicity of the compound was due to the physicochemical properties of the compound, especially poor aqueous solubility, rather than an intrinsic property of antifolate based TS inhibitors.[15,16]

Several studies have been carried out in which the effects of modifications to various parts of 1 were investigated.[17-28] In particular, the consequences on in vitro TS inhibition and tumor cell growth inhibition of changing the C2-amino group of the bicycle have been reported.[18-21,23] Replacement of this functional group of 1 with a hydrogen[18,20,27] or methyl[19,21] substituent led to compounds with greater aqueous solubility, a lack of liver and kidney toxicity in mice, and enhanced efficacy as inhibitors of tumor cell growth in vitro. Subsequently a large number of compounds with a variety of C2 substituents have been synthesized and evaluated as novel cancer cell growth inhibitors.[23] The effects of modifications to the N10 substituent[28] and the *p*-aminobenzoyl ring[22,25,26] have also been studied.

† ICI Pharmaceuticals.
‡ Institute of Cancer Research.

(1) Jones, T. R.; Calvert, A. H.; Jackman, A. L.; Brown, S. J.; Jones, M.; Harrap, K. R. A Potent Antitumour Quinazoline Inhibitor of Thymidylate Synthetase: Synthesis, Biological Properties, and Therapeutic Results in Mice. *Eur. J. Cancer* 1981, *17*, 11-19.
(2) Jackman, A. L.; Taylor, G. A.; O'Connor, B. M.; Bishop, J. A. M.; Moran, R. G.; Calvert, A. H. Activity of the Thymidylate Synthase Synthase Inhibitor 2-Desamino-N[10]-propargyl-5,8-dideazafolic acid and related Compounds in vitro and in L1210 in vivo. *Cancer Res.* 1990, *50*, 5212-5218.
(3) Jackman, A. L.; Calvert, A. H.; Hart, L. I.; Harrap, K. R. Inhibition of Thymidylate Synthase by the new Quinazoline Antifolate CB3717; Enzyme Purification and Kinetics. In *Purine Metabolism in Man-IV,165B*; DeBruyn, C. H. M. M., Simmonds, H. A., Muller, M., Eds.; Plenum Publishing Corp.: New York, 1984; pp 375-378.
(4) Jackson, R. C.; Jackman, A. L.; Calvert, A. H. Biochemical Effects of a Quinazoline Inhibitor of Thymidylate Synthase, CB3717, on Human Lymphoblastoid Cells. *Biochem. Pharmacol.* 1983, *32*, 3783-3790.
(5) Pogolotti, A. L.; Danenberg, P. V.; Santi, D. V. Kinetics and Mechanism of Interaction 10-propargyl-5,8-dideazafolate with Thymidylate Synthase. *J. Med. Chem.* 1986, *29*, 478-482.
(6) Cheng, Y.-C.; Dutschman, G. E.; Starnes, M. C.; Fischer, M. H.; Nanavathi, N. T.; Nair, M. G. Activity of the New Antifolate N[10]-propargyl-5,8-dideazafolate and its Polyglutamates Against Human Dihydrofolate Reductase, Human Thymidylate Synthase, and KB Cells Containing Different Levels of Dihydrofolate Reductase. *Cancer Res.* 1985, *45*, 598-600.
(7) Curtin, N. J.; Harris, A. L.; Jamer, O. F. W.; Bassendine, M. F. Inhibition of the Growth of Human Hepatocellular Carcinoma In Vitro and in Athymic Mice by a Quinazoline Inhibitor of Thymidylate Synthase, CB3717. *Br. J. Cancer* 1986, *53*, 361-368.

0022-2623/92/1835-2761$03.00/0